COMPUTATIONAL STUDY OF DRUG DELIVERY SYSTEMS WITH RADIONUCLIDE AND FLUORESCENCE IMAGING MODALITIES. II. DOXORUBICIN DELIVERY SYSTEMS BASED ON ALBUMIN AND TRANSFERRIN

V. Trusova[a]*, U. Malovytsia[a], P. Kuznietsov[b], I. Karnaukhov[c], A. Zelinsky[c], B. Borts[c], I. Ushakov[c], L. Sidenko[c], G. Gorbenko[a]

aDepartment of Medical Physics and Biomedical Nanotechnologies, V.N. Karazin Kharkiv National University
4 Svobody Sq., Kharkiv, 61022, Ukraine
bO.I. Akhiezer Department for Nuclear Physics and High Energy Physics, V.N. Karazin Kharkiv National University
4 Svobody Sq., Kharkiv, 61022, Ukraine
cNational Science Center "Kharkov Institute of Physics and Technology", Kharkiv, Ukraine
*Corresponding Author e-mail: valerija.trusova@karazin.ua

This study explores the development of advanced protein-based drug delivery systems for doxorubicin (DOX), an anticancer agent, incorporating both radionuclide (technetium-99m complexes) and fluorescence (Methylene Blue (MB), Indocyanine Green (IG), cyanine AK7-5 and squaraine SQ1) imaging modalities. Building upon previous research on albumin-based carriers, this work expands the scope by introducing transferrin (TRF) as a complementary protein component to create a more sophisticated and targeted delivery platform. Molecular docking technique was employed to design and characterize the multimodal delivery systems that incorporate radiopharmaceuticals and near-infrared fluorescent dyes. The results demonstrate that technetium-99m-based radiopharmaceuticals are capable of strong noncovalent binding to human serum albumin (HSA) and its complexes with transferrin. A comprehensive analysis of docking scores and interacting amino acid residues reveals that HSA-TRF-TcHyn/TcMEB/TcDIS-DOX-IG/SQ1 systems show the highest potential for experimental testing and further development. These findings support the potential of HSA-TRF complexes as nanocarriers with dual imaging capabilities for DOX delivery, offering an approach to enhance therapeutic efficacy while reducing systemic toxicity in anticancer treatment.

Keywords: *Drug delivery nanosystems; Human serum albumin; Transferrin; Doxorubicin; Technetium complexes; Fluorescent dyes; Molecular docking*
PACS: 87.14.C++c, 87.16.Dg

Protein-based drug delivery systems have emerged as a promising strategy for enhancing the therapeutic efficacy of anticancer agents while mitigating their systemic toxicity [1,2]. These systems offer exceptional biocompatibility, biodegradability, and the ability to accumulate in tumor tissues via the enhanced permeability and retention effect (EPR). Proteins, as drug delivery cargos, provide unique advantages such as natural abundance, renewable sources, and the presence of multiple functional groups for drug loading and targeting modifications [3,4]. In our previous paper we explored albumin-based drug delivery systems for doxorubicin (DOX) [5]. Accordingly, the study employed computational tools to design multimodal delivery systems incorporating radiopharmaceuticals and near-infrared fluorescent dyes, and the results obtained provided strong support for the ability of human serum albumin (HSA) as DOX delivery systems. Currently, the ongoing research in this field is focused on developing more sophisticated and efficient protein-based nanocarriers [6]. Motivated by these rationales, in the present paper we extend the scope of our research by introducing transferrin (TRF) as a complementary protein component to create a more sophisticated and targeted delivery platform. The combination of HSA and transferrin in a single delivery system aims to leverage the advantages of both proteins. While albumin provides excellent biocompatibility and drug-binding capabilities [7], transferrin adds an active targeting mechanism to cancer cells overexpressing transferrin receptors [8]. This dual-protein approach may result in improved drug accumulation in tumor tissues, not only through the EPR effect but also via receptor-mediated endocytosis.

METHODS

Human serum albumin (HSA) in its dimeric form (PDB ID: 1AO6) was used as a main component of the designed PDDS. A therapeutic component of the examined drug delivery systems was represented by one of the most widespread antitumor drug doxorubicin (DOX), anthracycline antibiotic whose antineoplastic properties arise mainly from its abilities to intercalate into DNA, inhibit topoisomerase II, disrupt gene expression, generate reactive oxygen species and produce damage of cell membranes [9]. To design the PDDS, in the present study we used 12 ^{99m}Tc-based radiopharmaceuticals [5]: [^{99m}Tc]Tc-Sestamibi (TcSES), [^{99m}Tc]Tc-Tetrofosmin (TcTET), [^{99m}Tc]Tc-Medronate (TcMED), [^{99m}Tc]Tc-

dimercaptosuccinic acid (TcDMSA), [^{99m}Tc]Tc-diethylenetriaminepentaacetate (Tc-DTPA), [^{99m}Tc]Tc-mercaptoacetyltriglycine (TcMAG), Pertechnetate [^{99m}Tc]TcO4− (TcPER), [^{99m}Tc]Tc-Exametazime (TcEXA), [^{99m}Tc]Tc-diisopropyl iminodiacetic acid (TcDIS), [^{99m}Tc]Tc-ethylene cysteine dimer (TcECD), [^{99m}Tc]Tc- hydrazinonicotinic acid-H6F (TcHYN), [^{99m}Tc]Tc-Mebrofenin (TcMEB). To create the dual-labelled PDDS with both nuclear and optical imaging modalities, the examined protein systems were loaded by the binary combinations of the above ^{99m}Tc complexes and four NIR fluorescent dyes (FD), Methylene Blue (MB), Indocyanine Green (IG), cyanine AK7-5 and squaraine SQ1 [5]. To identify the most energetically favorable binding sites for TCC, DOX, FD in the HSA-TRF protein systems the molecular docking studies were performed using the HDOCK server. Prior to the docking procedure, the structures of HSA dimers and its complexes with TRF were relaxed through 1 ns MD simulations. The structures of ligands were built in MarvinSketch (version 18.10.0) and the geometries were further optimized in Avogadro (version 1.1.0). The selected docking poses were visualized with the UCSF Chimera software (version 1.14) and analyzed with Protein-Ligand Interaction Profiler [10].

RESULTS AND DISCUSSION

In our previous paper we conducted sophisticated molecular docking studies to design the albumin-based drug delivery systems for DOX with dual imaging modalities, including the complexes of the radionuclide technetium-99m (TCC) and near-infrared (NIR) fluorescent dyes [5]. In brief, our computational analysis revealed that among the compounds studied, the technetium complexes TcDIS, TcHYN, and TcMEB exhibited the strongest binding affinities to the protein. Furthermore, molecular docking analysis indicated that the majority of TCCs preferentially bound to domain I of HSA, with some exceptions showing affinity for both domains I and III or exclusively for domain III.

In the present paper we aimed at answering the question of whether HSA association with other functional proteins, such as transferrin (TRF), can affect the TCC binding properties. Fig. 1 represents the best score complexes of TCC with HSA-TRF complexes.

A   B
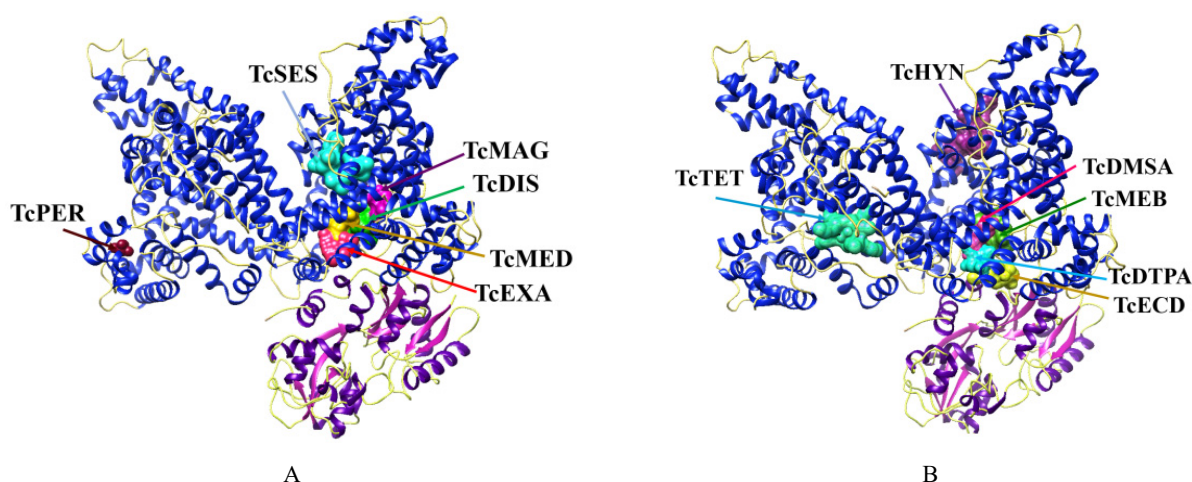
Figure 1. The most energetically favorable complexes of TCC with HSA-TRF complexes

In the hybrid protein systems, the best docking score (BDS) values were found to decrease in the row HSA + TRF - TcHYN > TcDIS > TcDTPA > TcMEB > TcDMSA > TcSES >TcTET ~ TcECD ~ TcMAG ~ TcMED ~ TcEXA > TcPER (Fig. 2). in all these systems the highest affinity was observed for TcHYN.
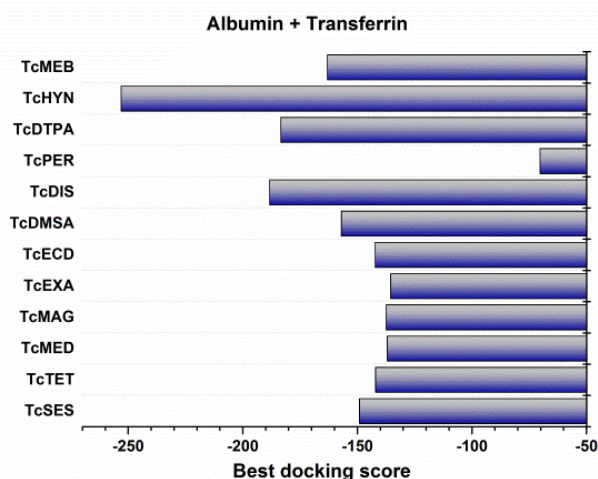
Figure 2. The best docking score values obtained for the TCC complexes with HSA and its associates with TRF

Notably, the BDS value for the neat HSA-TRF complexes (without TCC) was estimated to be -200.2, with the number of interface residues being equal to 62 (Table 1).

Table 1. The interface amino acid residues and the types of interactions involved in the binding of technetium-99m complexes (TCC) to the albumin-transferrin (TRF) associates

TCC	HSA-TRF-TCC interface residues		Type of interactions
	HSA	TRF	
TcSES	TYR_{150A*}, GLU_{153A}, PHE_{156A}, PHE_{157A}, ARG_{160A}, GLU_{188A}, ALA_{191A}, SER_{192A}, LYS_{195A}, GLN_{196A}, LYS_{199A}, ARG_{218A}, ARG_{222A}, HSD_{288A}, GLU_{292A}, VAL_{293A}, LYS_{436A}, HSD_{440A}, TYR_{452A}		Hydrophobic interactions, hydrogen bonds
TcTET	LEU_{115B}, ARG_{114B}, ARG_{145B}, LYS_{190B}, SER_{419B}, ARG_{428B}, ILE_{523B}, GLU_{540B}		Hydrophobic interactions, hydrogen bonds
TcMED	LEU_{115A}, ARG_{117A}, TYR_{138A}, ILE_{142A}, HSD_{146A}, PHE_{149A}, LEU_{154A}, PHE_{157A}, TYR_{161A}, LEU_{182A}, ASP_{183A}, LEU_{185A}, ARG_{186A}, ASP_{187A}, GLY_{189A}, LYS_{190A}		Hydrogen bonds
TcMAG	ASP_{107A}, ASP_{108A}, ASN_{109A}, ARG_{145A}, HSD_{146A}, PRO_{147A}, TYR_{148A}, GLY_{189A}, LYS_{190A}, ALA_{191A}, SER_{193A}, ALA_{194A}, ARG_{197A}, GLU_{425A}, ASN_{458A}, GLN_{459A}		Hydrogen bonds, salt bridges
TcEXA	LEU_{115A}, VAL_{116A}, ARG_{117A}, PRO_{118A}, MET_{123A}, PHE_{134A}, LYS_{137A}, TYR_{138A}, LEU_{139A}, GLU_{141A}, ILE_{142A}, ARG_{145A}, TYR_{161A}, PHE_{165A}, LEU_{182A}, ARG_{186A}		Hydrophobic interactions, hydrogen bonds
TcECD	GLN_{33A}, LEU_{112A}, PRO_{113A}, ARG_{114A}, LEU_{115A}, VAL_{116A}, ARG_{117A}, PRO_{118A}, TYR_{140A}, GLU_{141A}, ARG_{144A}, ARG_{145A}	TYR_{71}, LEU_{72}, ALA_{73}, ASN_{76}, LEU_{77}, LYS_{78}, PRO_{79}, SER_{255}, MET_{309}, ASP_{310}	Hydrophobic interactions, hydrogen bonds, salt bridges
TcDMSA	LEU_{115A}, VAL_{116A}, ARG_{117A}, PRO_{118A}, MET_{123A}, TYR_{138A}, ILE_{142A}, HSD_{146A}, PHE_{149A}, LEU_{154A}, PHE_{157A}, TYR_{161A}, LEU_{182A}, LEU_{185A}, ARG_{186A}, ASP_{187A}, GLU_{188A}, GLY_{189A}, LYS_{190A}		Hydrogen bonds, salt bridges
TcDIS	ASN_{109A}, ARG_{145A}, HSD_{146A}, ARG_{186A}, LYS_{190A}, PRO_{421A}, GLU_{425A}, GLU_{520A}	ARG_{308}	Hydrophobic interactions, hydrogen bonds, salt bridges
TcPER	TYR_{30B}, HSD_{67B}, THR_{68B}, PHE_{70B}, GLY_{71B}, LEU_{74B}, GLU_{95B}, ARG_{98B}, ASN_{99B}, PHE_{102B}		Hydrogen bonds
TcDTPA	LEU_{115A}, VAL_{116A}, ARG_{117A}, PRO_{118A}, MET_{123A}, PHE_{134A}, LEU_{135A}, LYS_{137A}, TYR_{138A}, GLU_{141A}, ILE_{142A}, TYR_{161A}, LEU_{182A}, ARG_{186A}		Hydrogen bonds, salt bridges
TcHYN	GLU_{383A}, LEU_{387A}, ASN_{391A}, LEU_{394A}, ALA_{406A}, LEU_{407A}, VAL_{409A}, ARG_{410A}, TYR_{411A}, LEU_{430A}, LEU_{453A}, SER_{489A}, GLU_{492A}, GLU_{542A}, LYS_{545A}		Hydrogen bonds, π-stacking, salt bridges
TcMEB	ASP_{108A}, ASN_{109A}, PRO_{110A}, ASN_{111A}, LEU_{112A}, PRO_{113A}, ARG_{114A}, LEU_{115A}, ARG_{145A}, HSD_{146A}, ARG_{186A}, LYS_{190A}, PRO_{421A}, THR_{422A}, VAL_{424A}, GLU_{425A}, ILE_{523A}, LYS_{524A}, THR_{527A}	ARG_{308}	Hydrophobic interactions, hydrogen bonds, salt bridges

The modification of the ligand binding landscape upon HSA complexation with TRF resulted in the changes of the binding affinity for some TCC. As illustrated in Fig. 3, the most pronounced affinity increase was observed for TcDIS and less pronounced – for TcMED.

In the HSA-TRF systems the binding sites most TCC reside solely on the albumin molecule, only TcECD, TcMEB and TcDIS interact with both proteins, HSA and TRF (Fig. 1, Table 1). Interestingly, despite TcDIS makes contacts with

only one TRF residue, ARG308, this seems to play a role in the increase of TcDIS affinity in the presence of transferrin compared to HSA alone.
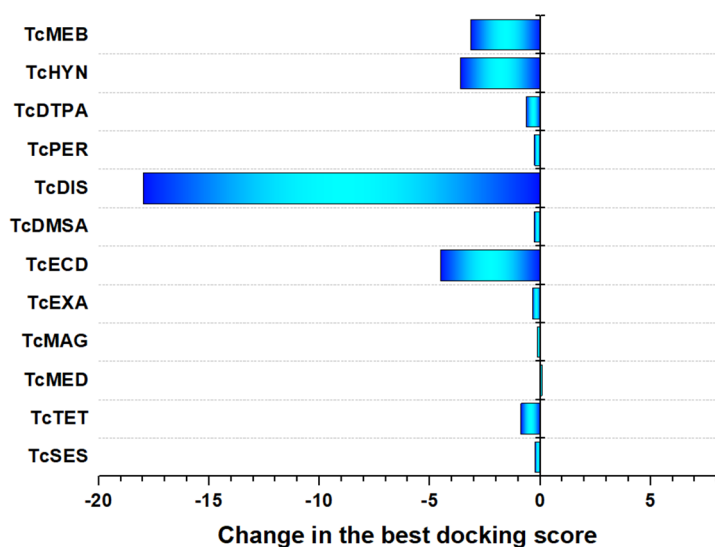
Figure 3. The changes in the best docking score values calculated for HSA-TRF-TCC systems relative to HSA alone

Next, we employed the multiple ligands docking approach to explore the ternary protein-ligand systems (HSA-TRF-TCC-DOX). The ternary systems were obtained by the docking of doxorubicin to the best score complexes of TCC with HSA-TRF (Fig. 4).
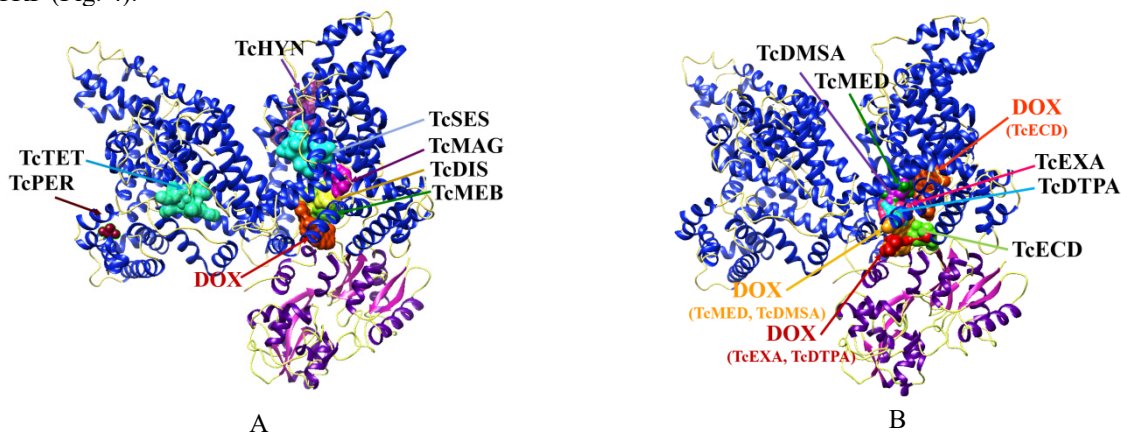
Figure 4. The most energetically favorable complexes of TCC with HSA-TRF complexes

The following features of the ternary systems are worthy of mention: i) in most HSA-TRF-TCC-DOX systems (except TcECD), the DOX protein affinities are higher than those for the HSA-TCC-DOX systems, ii) all DOX binding sites constitute the residues from both HSA (most residues from the site HSA$_{113-186}$) and TRF (predominantly TYR$_{71}$, LEU$_{72}$, ALA$_{73}$ and ASN$_{76}$) (Table 2).

Table 2. The interface amino acid residues and the types of interactions involved in the binding of DOX to HSA-TRF-TCC complexes

Complex	HSA-TRF-TCC-DOX- interface residues		Type of interactions
	HSA	TRF	
HSA-TRF-DOX	LEU$_{112A}$*, PRO$_{113A}$, ARG$_{114A}$, LEU$_{115A}$, VAL$_{116A}$, ARG$_{117A}$, PRO$_{118A}$, MET$_{123A}$, PHE$_{134A}$, LYS$_{137A}$, TYR$_{138A}$, GLU$_{141A}$, ARG$_{145A}$, TYR$_{161A}$, LEU$_{182A}$, ARG$_{186A}$	TYR$_{71}$, LEU$_{72}$, ALA$_{73}$, ASN$_{76}$	Hydrophobic interactions, hydrogen bonds, π-stacking, π-cation interactions, salt bridges
HSA-TRF-TcSES-DOX	LEU$_{112A}$, PRO$_{113A}$, ARG$_{114A}$, LEU$_{115A}$, VAL$_{116A}$, ARG$_{117A}$, PRO$_{118A}$, MET$_{123A}$, PHE$_{134A}$, LYS$_{137A}$, TYR$_{138A}$, GLU$_{141A}$,	TYR$_{71}$, LEU$_{72}$, ALA$_{73}$, ASN$_{76}$	Hydrophobic interactions, hydrogen bonds, π-stacking, π-cation

Complex	HSA-TRF-TCC-DOX- interface residues		Type of interactions
	HSA	**TRF**	
	ARG_{145A}, TYR_{161A}, LEU_{182A}, ARG_{186A}		interactions, salt bridges
HSA-TRF-TcTET-DOX	LEU_{112A}, PRO_{113A}, ARG_{114A}, LEU_{115A}, VAL_{116A}, ARG_{117A}, PRO_{118A}, MET_{123A}, PHE_{134A}, LYS_{137A}, TYR_{138A}, GLU_{141A}, ARG_{145A}, TYR_{161A}, LEU_{182A}, ARG_{186A}	TYR_{71}, LEU_{72}, ALA_{73}, ASN_{76}	Hydrophobic interactions, hydrogen bonds, π-stacking, π-cation interactions, salt bridges
HSA-TRF-TcMED-DOX	PRO_{113A}, ARG_{114A}, LEU_{115A}, VAL_{116A}, ARG_{117A}, PRO_{118A}, MET_{123A}, ALA_{126A}, PHE_{134A}, LYS_{137A}, TYR_{138A}, GLU_{141A}, ILE_{142A}, ARG_{145A}, TYR_{161A}	TYR_{68}, TYR_{71}, LEU_{72}, ALA_{73}, ASP_{310}, ALA_{311}, LYS_{312}, VAL_{320}, ARG_{324}	Hydrophobic interactions, hydrogen bonds, π-cation interactions, salt bridges
HSA-TRF-TcMAG-DOX	LEU_{112A}, PRO_{113A}, ARG_{114A}, LEU_{115A}, VAL_{116A}, ARG_{117A}, PRO_{118A}, MET_{123A}, PHE_{134A}, LYS_{137A}, TYR_{138A}, GLU_{141A}, ARG_{145A}, TYR_{161A}, LEU_{182A}, ARG_{186A}	TYR_{71}, LEU_{72}, ALA_{73}, ASN_{76}	Hydrophobic interactions, hydrogen bonds, π-stacking, π-cation interactions, salt bridges
HSA-TRF-TcEXA-DOX	LEU_{112A}, PRO_{113A}, ARG_{114A}, LEU_{115A}, VAL_{116A}, ARG_{117A}, PRO_{118A}, VAL_{122A}, LYS_{137A}, GLU_{141A}, ARG_{144A}, ARG_{145A}	TYR_{68}, TYR_{71}, LEU_{72}, ALA_{73}, ASN_{76}, ASP_{310}, ALA_{311}, LYS_{312}, VAL_{320}, ARG_{324}, GLU_{328}	Hydrophobic interactions, hydrogen bonds, π-cation interactions, salt bridges
HSA-TRF-TcECD-DOX	ASP_{107A}, ASP_{108A}, ASN_{109A}, PRO_{110A}, ASN_{111A}, LEU_{112A}, PRO_{113A}, ARG_{114A}, ARG_{145A}, HSD_{146A}, PRO_{147A}, TYR_{148A}, LYS_{190A}, SER_{193A}, ALA_{194A}, ARG_{197A}, PRO_{421A}, THR_{422A}, GLU_{425A}, GLN_{459A}	ARG_{308}	Hydrophobic interactions, hydrogen bonds
HSA-TRF-TcDMSA-DOX	PRO_{113A}, ARG_{114A}, LEU_{115A}, VAL_{116A}, ARG_{117A}, PRO_{118A}, MET_{123A}, ALA_{126A}, PHE_{134A}, LYS_{137A}, TYR_{138A}, GLU_{141A}, ILE_{142A}, ARG_{145A}, TYR_{161A}	TYR_{68}, TYR_{71}, LEU_{72}, ASP_{310}, ALA_{311}, LYS_{312}, VAL_{320}, ARG_{324}	Hydrophobic interactions, hydrogen bonds, π-cation interactions, salt bridges
HSA-TRF-TcDIS-DOX	LEU_{112A}, PRO_{113A}, ARG_{114A}, LEU_{115A}, VAL_{116A}, ARG_{117A}, PRO_{118A}, MET_{123A}, PHE_{134A}, LYS_{137A}, TYR_{138A}, GLU_{141A}, ARG_{145A}, TYR_{161A}, LEU_{182A}, ARG_{186A}	TYR_{71}, LEU_{72}, ALA_{73}, ASN_{76}	Hydrophobic interactions, hydrogen bonds, π-stacking, π-cation interactions, salt bridges
HSA-TRF-TcPER-DOX	LEU_{112A}, PRO_{113A}, ARG_{114A}, LEU_{115A}, VAL_{116A}, ARG_{117A}, PRO_{118A}, MET_{123A}, PHE_{134A}, LYS_{137A}, TYR_{138A}, GLU_{141A}, ARG_{145A}, TYR_{161A}, LEU_{182A}, ARG_{186A}	TYR_{71}, LEU_{72}, ALA_{73}, ASN_{76}	Hydrophobic interactions, hydrogen bonds, π-stacking, π-cation interactions, salt bridges
HSA-TRF-TcDTPA-DOX	LEU_{112A}, PRO_{113A}, ARG_{114A}, LEU_{115A}, VAL_{116A}, ARG_{117A}, PRO_{118A}, VAL_{122A}, LYS_{137A}, GLU_{141A}, ARG_{144A}, ARG_{145A}	TYR_{68}, TYR_{71}, LEU_{72}, ALA_{73}, ASN_{76}, ASP_{310}, ALA_{311}, LYS_{312}, VAL_{320}, ARG_{324}, GLU_{328}	Hydrophobic interactions, hydrogen bonds, π-cation interactions, salt bridges
HSA-TRF-TcHYN-DOX	LEU_{112A}, PRO_{113A}, ARG_{114A}, LEU_{115A}, VAL_{116A}, ARG_{117A}, PRO_{118A}, MET_{123A}, PHE_{134A}, LYS_{137A}, TYR_{138A}, GLU_{141A}, ARG_{145A}, TYR_{161A}, LEU_{182A}, ARG_{186A}	TYR_{71}, LEU_{72}, ALA_{73}, ASN_{76}	Hydrophobic interactions, hydrogen bonds, π-stacking, π-cation interactions, salt bridges
HSA-TRF-TcMEB-DOX	LEU_{112A}, PRO_{113A}, ARG_{114A}, LEU_{115A}, VAL_{116A}, ARG_{117A}, PRO_{118A}, MET_{123A}, PHE_{134A}, LYS_{137A}, TYR_{138A}, GLU_{141A}, ARG_{145A}, TYR_{161A}, LEU_{182A}, ARG_{186A}	TYR_{71}, LEU_{72}, ALA_{73}, ASN_{76}	Hydrophobic interactions, hydrogen bonds, π-stacking, π-cation interactions, salt bridges

*-A and B denote monomer subunits of the HSA dimer

In the following, to develop systems with dual imaging capabilities, we expanded our computational analysis by incorporating near-infrared (NIR) fluorophores into the highest-scoring protein-TCC-DOX complexes. This approach involved docking four distinct NIR fluorescent dyes to these complexes. We selected two conventional fluorophores, methylene blue and indocyanine green, along with two novel fluorescent agents, heptamethine cyanine dye AK7-5 and squaraine dye SQ1.
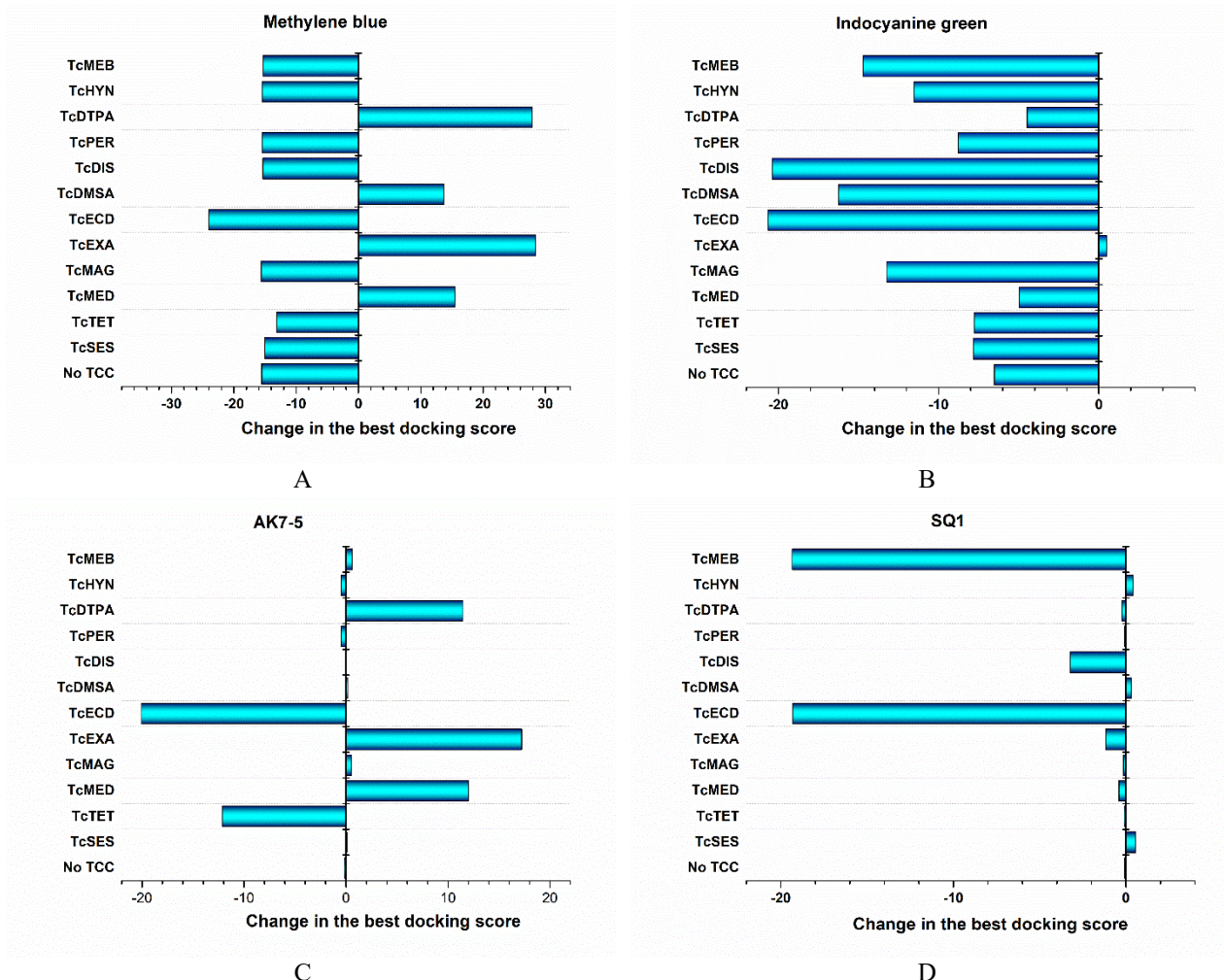
Figure 5. The changes in the best docking score values calculated for HSA-TRF-TCC-DOX-FD systems relative to the systems HSA-TCC-DOX-FD

By integrating these NIR fluorophores, we aimed to create multimodal imaging systems that combine the advantages of radionuclide-based imaging (via technetium complexes) with the high sensitivity and spatial resolution of NIR fluorescence imaging. A comprehensive evaluation of the docking results for the quaternary systems (protein + TCC + DOX + FD) reveals a clear trend in the binding affinities of the examined fluorescent dyes to HSA and HSA-DOX complexes [5]. The affinity decreases in the following order: indocyanine green (IG) > squaraine dye (SQ1) > heptamethine cyanine dye (AK7-5) > methylene blue (MB). This trend is evidenced by their respective BDS. While the specific amino acid residues involved in FD binding sites vary across different TCC and protein components, certain patterns emerge for each system. Notably, a consistent binding site for MB was identified in HSA-DOX, HSA-TCC-DOX, and HSA-TRF-DOX complexes. This site, designated as $HSA_{115-186}$, comprises 12 amino acid residues between LEU_{115} and ARG_{186} of albumin. Interestingly, in most HSA-TRF-TCC-DOX systems, the MB binding sites are composed of residues from both proteins in the complex. This suggests a cooperative binding mechanism involving multiple protein components. Furthermore, the addition of TRF to the HSA systems generally enhances MB binding affinity compared to HSA alone (Fig. 5, A).

The analysis of HSA binding sites for IG in HSA-TRF-TCC-DOX systems reveals the existence of three amino acid residues - ARG_{114A}, PRO_{421A}, and ILE_{523A} that are present in IG binding sites on HSA. The fluorescent dye AK7-5 interacts with HSA through sites composed of 18 (site $HSA_{115-523}$) or 12 amino acid residues from albumin domains I and III. Significant increases in binding affinity were observed in HSA-Lz-TcTET-DOX systems (Fig. 5, C) where AK7-5 binds either to the $HSA_{115-523}$ site or to hybrid sites of varying composition. Interestingly, in HSA-Lz/TRF complexes SQ1 binds to a site on HSA ($HSA_{115-523}$) supplemented by an additional residue (ASP_{173A}) from another albumin monomer. Overall, addition of TRF as second protein component gave rise to the substantial changes in BDS for MB and

IG as compared to the systems where protein was represented only by HSA (Fig. 5). In the case of AK7-5 and SQ1, the most pronounced changes in BDS were observed for TcECD.

CONCLUSIONS

In conclusion, the present study has been undertaken to verify the idea that the human serum albumin and its complexes with transferrin can be employed to create the nanocarriers with dual imaging capabilities for the antitumor drug doxorubicin. The results obtained showed that TcHYN, TcDIS, TcMEB and TcDTPA are capable of strong noncovalent binding to HSA and HSA-Lz/TRF/Hb complexes. Comprehensive analysis of best docking score values along with the interacting amino acid residues allows recommending HSA-TRF-TcHyn/TcMEB/TcDIS-DOX-IG/SQ1 systems as the most promising for experimental testing and further development of the protein-based nanoscale systems for DOX delivery with dual imaging functionalities.

ORCID

Valeriya Trusova, https://orcid.org/0000-0002-7087-071X; **Uliana Malovytsia,** https://orcid.org/0000-0002-7677-0779
Galyna Gorbenko, https://orcid.org/0000-0002-0954-5053; **Andrey Zelinsky,** https://orcid.org/0000-0002-4110-8523
Borys Borts, https://orcid.org/0000-0002-1492-4066; **Pylyp Kuznietsov,** https://orcid.org/0000-0001-8477-1395

REFERENCES

[1]   C. Ferraro, M. Dattilo, F. Patitucci, S. Prete, G. Scopelliti, O. Parisi, and F. Puoci, Pharmaceutics. **16**, 1172 (2024). https://doi.org/10.3390/pharmaceutics16091172
[2]   S. Hong, D. Choi, H. Kim, C. Park, W. Lee, and H. Park, Pharmaceutics. **12**, 604 (2020). https://doi.org/10.3390/pharmaceutics12070604
[3]   A. Gorantla, J. Hall, A. Troidle, and J. Janjic, Micromachines **15**, 533 (2024). https://doi.org/10.3390/mi15040533
[4]   M. Larsen, M. Kuhlmann, M. Hvam, and K. Howard, Mol. Cell Ther. **4**, 3 (2016). https://doi.org/10.1186/s40591-016-0048-8
[5]   V. Trusova, U. Tarabara, I. Karnaukhov, A. Zelinsky, B. Borts, I. Ushakov, L. Sidenko, and G. Gorbenko, East Eur. J. Phys. (4), 447 (2024). https://doi.org/10.26565/2312-4334-2024-4-54
[6]   M. Puccetti, M. Pariano, A. Schoubben, S. Giovagnoli, and M. Ricci, Pharmacol Res. **201**, 107086 (2024). https://doi.org/10.1016/j.phrs.2024.107086
[7]   N. Qu, K. Song, Y. Ji, M. Liu, L. Chen, R. Lee, and L. Teng, Int. J. Nanomedicine. **19**, 6945 (2024). https://doi.org/10.2147/IJN.S467876
[8]   H. Choudhury, M. Pandey, P. Chin, Y. Phang, J. Cheah, S. Ooi, K. Mak, *et al*., Drug Deliv Transl Res. **8**, 1545 (2018). https://doi.org/10.1007/s13346-018-0552-2
[9]   M. Kciuk, A. Gielecinska, S. Mujwar, D. Kołat, Z. Kałuzinska-Kołat, I. Celik, and R. Kontek, Cells. **12**, 659 (2023). https://doi.org/10.3390/cells12040659
[10] M. F. Adasme, K. L. Linnemann, S. N. Bolz, F. Kaiser, S. Salentin, V. J. Haupt, and M. Schroeder, Nucl. Acids Res. **49**, W530-W534 (2021). https://doi.org/10.1093/nar/gkab294

КОМП'ЮТЕРНЕ ДОСЛІДЖЕННЯ СИСТЕМ ДОСТАВКИ ЛІКІВ З РАДІОНУКЛІДНИМИ ТА ФЛУОРЕСЦЕНТНИМИ МОДАЛЬНОСТЯМИ ВІЗУАЛІЗАЦІЇ. ІІ. СИСТЕМИ НА ОСНОВІ АЛЬБУМІНУ ТА ТРАНСФЕРИНУ ДЛЯ ДОСТАВКИ ДОКСОРУБІЦИНУ

В. Трусова[a], У. Маловиця[a], П. Кузнєцов[b], І. Карнаухов[c], А. Зелінський[c], Б. Борц[c], І. Ушаков[c], Л. Сіденко[c], Г. Горбенко[a]

[a]Кафедра медичної фізики та біомедичних нанотехнологій, Харківський національний університет імені В.Н. Каразіна м. Свободи 4, Харків, 61022, Україна
[b]Кафедра фізики ядра та високих енергій імені О.І. Ахієзера, Харківський національний університет імені В.Н. Каразіна м. Свободи 4, Харків, 61022, Україна
[c]Національний науковий центр «Харківський фізико - технічний інститут», Харків, вул. Академічна, 1, 61108, Україна

Дослідження присвячене розробці вдосконалених систем на основі білків для доставки лікарських засобів, зокрема, доксорубіцину (DOX) - протипухлинного агента, з інтеграцією радіонуклідних (комплекси технецію-99m) та флуоресцентних (метиленовий блакитний (МВ), індоціанін зелений (IG), ціаніновий барвник АК7-5 та сквараїновий барвник SQ1) модальностей. Базуючись на наших попередніх дослідженнях, в яких білкова компонента наноперносників була представлена альбуміном, в даній роботі трансферин (TRF) було застосовано як комплементарну білкову складову для створення більш складної та таргет-специфічної платформи доставки. Метод молекулярного докінгу було застосовано для дизайну та характеризації мультимодальних систем доставки, що включають радіофармпрепарати та флуоресцентні барвники ближнього інфрачервоного спектру. Отримані результати показали, що радіофармпрепарати на основі технецію-99m зв'язуються за допомогою нековалентних зв'язків з людським сироватковим альбуміном (HSA) та його комплексами з трансферином. Комплексний аналіз даних докінгу та амінокислотних залишків, що беруть участь у взаємодії, виявив, що системи HSA-TRF-TcHyn/TcMEB/TcDIS-DOX-IG/SQ1 демонструють найбільш високий потенціал для експериментальної верифікації та подальшої розробки. Ці дані свідчать, що комплекси HSA-TRF є перспективними наноносіями з подвійною візуалізацією для доставки DOX, які характеризуються підвищенням терапевтичної ефективності при одночасній мінімізації системної токсичності в онкотерапії.
Ключові слова: *наносистеми доставки ліків; людський сироватковий альбумін; трансферин; доксорубіцин; комплекси технецію; флуоресцентні барвники; молекулярний докінг*